



OPEN ACCESS

EDITED BY

Shangbin Xiao,
China Three Gorges University, China

REVIEWED BY

Xiangzhong Li,
Yunnan University, China
Xiumei Li,
Xinyang Normal University, China
Izabela Zawiska,
Polish Academy of Sciences, Poland

*CORRESPONDENCE

Yanling Li,
✉ yanlingli@ynu.edu.cn
Xiayun Xiao,
✉ xyxiao@niglas.ac.cn

RECEIVED 20 October 2023

ACCEPTED 19 January 2024

PUBLISHED 07 February 2024

CITATION

Zhang Y, Peng W, Li Y, Xiao X and Hillman A (2024), Diatom-based inferences of environmental changes from an alpine lake on the southeast edge of the Tibetan plateau over the last 4000 years. *Front. Earth Sci.* 12:1324724. doi: 10.3389/feart.2024.1324724

COPYRIGHT

© 2024 Zhang, Peng, Li, Xiao and Hillman. This is an open-access article distributed under the terms of the [Creative Commons Attribution License \(CC BY\)](https://creativecommons.org/licenses/by/4.0/). The use, distribution or reproduction in other forums is permitted, provided the original author(s) and the copyright owner(s) are credited and that the original publication in this journal is cited, in accordance with accepted academic practice. No use, distribution or reproduction is permitted which does not comply with these terms.

Diatom-based inferences of environmental changes from an alpine lake on the southeast edge of the Tibetan plateau over the last 4000 years

Yunxia Zhang¹, Wei Peng², Yanling Li^{3*}, Xiayun Xiao^{4*} and Aubrey Hillman⁵

¹School of Economics and Management, Suzhou Chien-Shiung Institute of Technology, Suzhou, China, ²School of Geography and Land Engineering, Yuxi Normal University, Yuxi, China, ³School of Ecology and Environment Science, Institute for Ecological Research and Pollution Control of Plateau Lakes, Yunnan University, Kunming, China, ⁴State Key Laboratory of Lake Science and Environment, Nanjing Institute of Geography and Limnology, Chinese Academy of Sciences, Nanjing, China, ⁵Department of Atmospheric and Environmental Sciences, University at Albany, State University of New York, Albany, NY, United States

To better understand how global and regional-scale climate has changed, high-resolution records for environmental changes are still needed in southwestern (SW) China during the Late Holocene epoch. This study presents a well-dated high-resolution diatom analysis from a 1.66-m-long sediment core taken from Lake Cuogeda (CGD) on the southeast (SE) edge of the Tibetan Plateau to document environmental changes over the past ~4000 years. Diatom and other geochemical proxies show that, from 3850 to 3430 cal yr BP (before present, 0 BP=1950 AD, 1900 to 1480 BC), the environment of Lake CGD is acidic, oligotrophic, and enriched with humic acids. And the lake ice cover duration is short during this period. During 3430–1550 cal yr BP (1480 BC–400 AD), Lake CGD has less humic acid and a relatively high pH environment. The ice cover duration is longer, and the temperature drops during this period. Our multi-indicator recorded two environment fluctuations at ~2800 cal yr BP (850 BC) and 2210–1950 cal yr BP (260 BC–0 AD). From 1550 to 3.6 cal yr BP (400–1946 AD), the lake ecosystem changed to a higher pH condition and had a prolonged freezing time. From 3.6 cal yr BP (1946 AD) to the present, Lake CGD's water was acidic, with an environment of shorter duration of ice cover and stronger lake water turbulence. Comparisons between the CGD records and other climate reconstructions underscore the relevance of the CGD record for regional and global environments. Comparisons indicate that the environment evolution pattern of SW China during the Late Holocene was greatly affected by solar radiation and North Atlantic sea surface temperature.

KEYWORDS

late holocene, climate change, diatoms, southwest China, southeast Tibetan plateau

1 Introduction

To better understand how the global and regional-scale climate has changed during the Holocene, it is essential to conduct paleoenvironment research with sufficient spatiotemporal resolution. The southeast (SE) margin of the Tibetan Plateau is one of the most environmentally sensitive regions to the Indian summer monsoon (ISM) change (An et al., 2011; Chen et al., 2015). The ISM is one of the most important subsystems of the monsoon climate system, which is critical to understanding the global energy cycle (Gupta et al., 2005). Understanding the variability of the ISM is essential not only for understanding global atmospheric circulation and climate change but also for preventing and mitigating disasters and achieving sustainable development (An et al., 2011).

The ISM variability over the Late Holocene has long been a critical focus for paleoclimatic reconstructions because the essential boundary conditions of Earth's climate are broadly comparable to those of the present day (Li et al., 2022). Variations in climate observed over this time interval likely represent the natural climate variability that might be expected during the present century without human influence. In the past decades, critical advances in paleoclimate studies of the Late Holocene in the Tibetan Plateau and its surrounding areas with various types of proxies have been achieved (e.g., Hong et al., 2003; Kramer et al., 2010; Wang et al., 2010; Chen et al., 2014; Bird et al., 2014; Xu et al., 2015; Hillman et al., 2017; Zhang et al., 2017; Li et al., 2018; Hillman et al., 2022; Zhang et al., 2023). However, there are contradictions among proxy climate reconstructions from the eastern and SE Tibetan Plateau region over the Late Holocene. For example, summer temperature reconstructed by alkenones from Hurlig Lake in the Qaidam Basin (Zhao et al., 2013) and BrGDGTs-based mean annual air temperature records from the Hongyuan peatland in the eastern Tibetan Plateau showed long-term climatic warming in the past 4000 years ago (Zheng et al., 2015). However, the chironomid-based record from Tiancai Lake on the SE margin of the Tibetan Plateau and a synthesis of fossil pollen records from the Tibetan Plateau indicate a cooling trend in summer temperature during the Late Holocene (Zhang et al., 2017; Chen et al., 2020). Moreover, conflicting results have been obtained using different lake sediment proxies for climate reconstructions of the same lake. The varve-thickness record of sediments from Kusai Lake on the northeastern Tibetan Plateau exhibits two warm periods during 600–720 AD and 800–1100 AD and a cold period during 1250–1760 AD (Liu et al., 2014). However, fossil pollen assemblages (Cui et al., 2021) and GDGTs (Wu et al., 2013) from the same lake indicate a cold period during 600–1100 AD and just a warm period during 1250–1750 AD. The GDGT reconstruction also shows that the past century was the warmest interval of the past two millennia at Kusai Lake. However, such unprecedented warming is not reflected by the fossil pollen assemblages (Cui et al., 2021) or the varve-thickness record (Liu et al., 2014). Thus, our understanding of the spatial patterns of climate change over the Tibetan Plateau during the Late Holocene is currently limited.

This study presents a high-resolution diatom analysis from an alpine lake over the past 4000 years. Climate change is assumed to be the primary cause of ecosystem shifts in alpine lakes since subtle variations in climate have a significant influence on organisms that

live in sensitive remote alpine lakes (Sommaruga-Wögrath et al., 1997; Koinig et al., 2002; Salmaso, 2005; Fritz and Anderson, 2013; Jiménez et al., 2019). Therefore, past changes in aquatic ecosystems can record climate information, especially for organismal groups that show a solid present-day relationship with climatic parameters (Lotter et al., 2010). Diatoms (Bacillariophyceae), one of the main groups of primary producers and photosynthetic protists in lakes, have multiple life strategies, specific ecological preferences, and short life spans, making them sensitive to environmental changes and, hence, the most extensively used biological indicators in paleolimnological studies (Stoermer and Smol, 1999; Rühland et al., 2003). It has been proven that diatom-based environment reconstruction in high-altitude lakes can be successfully used to track past climate changes (e.g., Bigler et al., 2003; Larocque and Bigler, 2004; Von Gunten et al., 2008; Lotter et al., 2010). Here, we present a high-resolution diatom analysis over the past 4000 years from Lake Cuogeda (28°03'09.42"N, 100°01'16.80"E; 4251 m a.s.l.), Yunnan Province, southwestern (SW) China (Figure 1). This record has an average temporal resolution of ~24 years, allowing for a detailed study of climate on centennial to millennial timescales. We will discuss the relationship between the diatom assemblages and the climate and environment changes during the Late Holocene and explain whether solar radiation and North Atlantic sea surface temperature may be the driving mechanisms.

2 Regional setting

Lake Cuogeda is located in an area of quartz syenite bedrock in the Hengduan Mountains of Yunnan on the SE edge of the Tibetan Plateau (28°03'09.42"N, 100°01'16.80"E; 4251 m a.s.l.). It is a small (about 12,247 m²), shallow lake (mean water depth of 2.5 m, Figures 1A, B). The chemical composition of the bedrock is characterized by high proportions of SiO₂ (71.3%–73.4%) and total alkali (K₂O+Na₂O, 7.4%–8.8%) (Ma, 2013). The soil type in the catchment is brown podzolic soil, with a mean pH of 4.03, organic matter of 177 mg g⁻¹, total nitrogen of 11 mg g⁻¹, total phosphorus of 1 mg g⁻¹, and total potassium of 10 mg g⁻¹ (Shi, 2007). Based on measurements taken at the lake in October 2016, Lake Cuogeda is weakly acidic (pH 6.86). The sediment at the bottom of the lake is mainly gray–black silt. The lake is surrounded by high mountains without human settlement and recharged by precipitation and meltwater without permanent inflows or outflows. It is a small freshwater glacial lake characterized by low water temperatures, extended periods of ice cover, low nutrient concentrations, and being fishless but with aquatic grasses. The lake water usually starts to freeze from October to November and melts from April to May.

The region belongs to the cold temperate zone and is controlled by the ISM, with warm wet summers and cold dry winters (Yao et al., 2017). Meteorological data from the Deqen meteorological station (3319 m a.s.l., meteorological data from National Meteorological Science Data Center, China), which is 117.5 km from Cuogeda Lake, show that the mean annual air temperature (MAT) is 5.86°C, with the lowest and highest mean monthly temperatures occurring in January (–1.8°C) and July (13°C), respectively (Figure 1C). The mean annual precipitation is

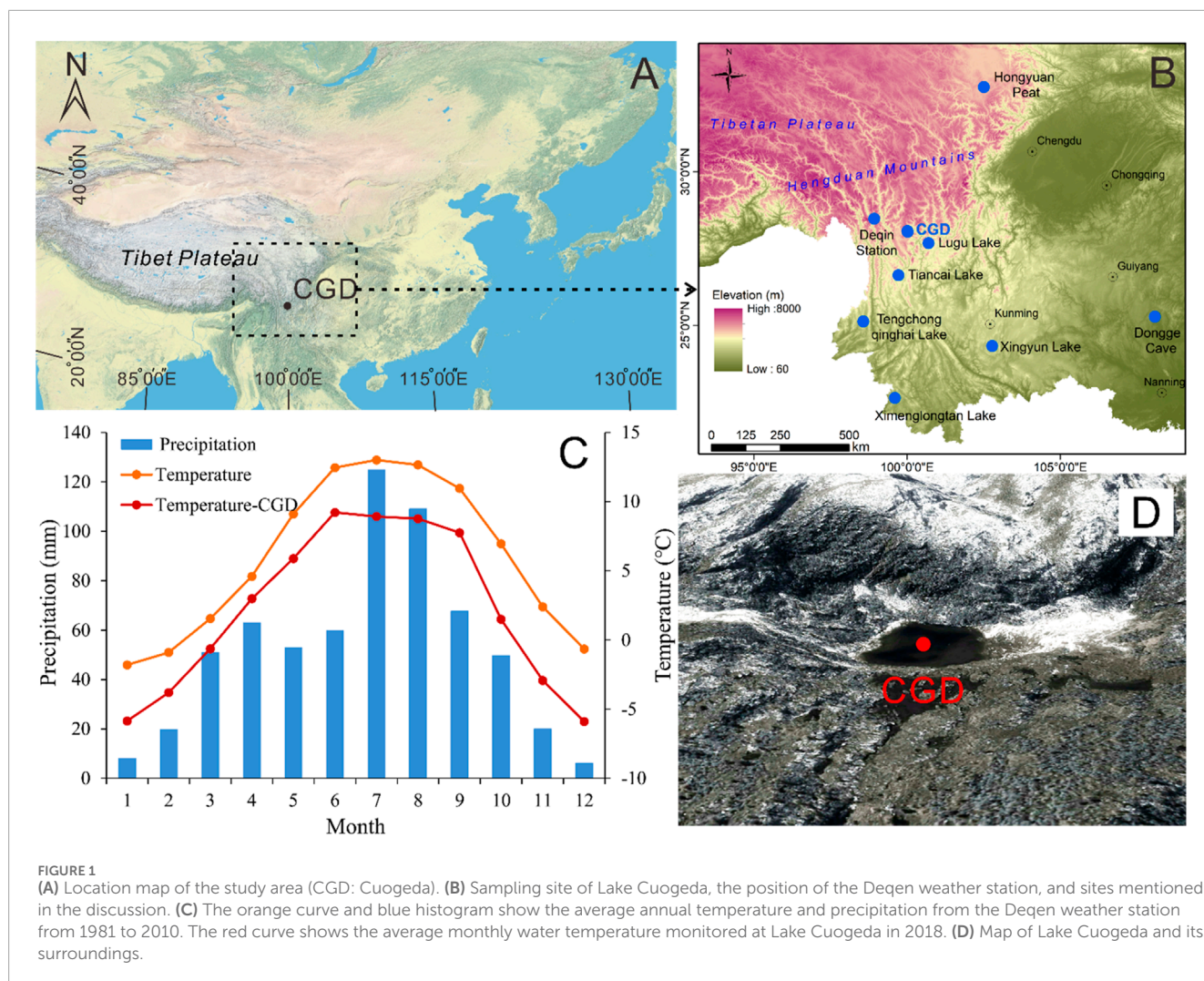


FIGURE 1 (A) Location map of the study area (CGD: Cuogeda). (B) Sampling site of Lake Cuogeda, the position of the Deqen weather station, and sites mentioned in the discussion. (C) The orange curve and blue histogram show the average annual temperature and precipitation from the Deqen weather station from 1981 to 2010. The red curve shows the average monthly water temperature monitored at Lake Cuogeda in 2018. (D) Map of Lake Cuogeda and its surroundings.

631 mm, with more than 37% falling between July and August (Figure 1C). Monitoring mean water temperature results at Lake Cuogeda in 2018 show a similar pattern to the MAT measured by the National Meteorological Science Data Center, China (Figure 1C). Vertical vegetation belts in the region are apparent: 1) 3100–3900 m a.s.l. (the forest line): subalpine cold-temperate conifer forest, with *Abies* and *Picea* as the dominant species; 2) 3900–5000 m a.s.l. (the snowline): alpine shrub, alpine meadow, and alpine tundra (Wu et al., 1987; Xiao et al., 2011). Lake Cuogeda is now above the tree line.

3 Materials and methods

3.1 Coring and radiocarbon dating

In October 2016, a 166-cm-long sediment core (CGD) was retrieved using a UWITEC piston corer from the central part of Lake Cuogeda (Figure 1B). It was then sectioned at 1-cm intervals and kept at 4°C for further analysis. Five terrestrial plant remains and 1 moss were selected for AMS ^{14}C dating

in the Poznań Radiocarbon Laboratory (Poland). All dates were calibrated to calendar years before the present (BP, 0 BP = 1950 AD) using the program CALIB 8.2 and IntCal20 calibration curve (Stuiver et al., 2020).

3.2 Diatom analysis

Diatom samples from the core of CGD were analyzed at 1-cm intervals and prepared following standard procedures (Battarbee et al., 2002). A total of 166 diatom samples were analyzed using an Olympus BX51 microscope with an oil immersion objective (magnification $\times 1000$). A minimum of 500 and an average of 803 valves were counted per sample. Diatom species were identified mainly according to Krammer and Lange-Bertalot (1986), Krammer and Lange-Bertalot (1988), and Krammer and Lange-Bertalot, 1991a; Krammer and Lange-Bertalot, 1991b).

Relative abundances of individual diatom species were calculated by dividing the number of valves from each species by the total sum of valves. To minimize the impact of rare species,

TABLE 1 AMS¹⁴C dates for the core CGD from Lake Cuogeda.

Lab code	Depth (cm)	Materials	¹⁴ C date (yr BP)	Calibrated age (cal yr BP, 2σ)	Median calibrated age (cal yr BP)
Poz-94614	30	Plant remains	200 ± 30	151–437	294
Poz-78614	54	Plant remains	880 ± 30	692–918	805
Poz-78615	77	Plant remains	1600 ± 30	1298–1592	1445
Poz-94615	107	Plant remains	2460 ± 30	2233–2643	2438
Poz-78616	141	Plant remains	2815 ± 35	2830–3228	3029
Poz-112302	165	Moss	3605 ± 35	3529–4022	3775.5

Poz: Poznań Radiocarbon Laboratory.

only diatom species with abundances >2% in at least two samples were retained in numerical analysis. Diatom diagrams were plotted using Tilia 2.6.1 (Grimm, 2004), and diatom assemblage zones were defined based on CONISS analysis of the diatom data (Grimm, 1987).

A prior evaluation based on detrended correspondence analysis (DCA) results could help determine whether linear or unimodal-based techniques should be employed in subsequent ordination analysis. Statistical analyses were based on diatom taxa (relative abundances) that occurred in at least two samples with an abundance >2%. The length of the gradient was less than two standard deviation (SD) units, and therefore, the principal component analysis (PCA) method was recommended to analyze the diatom assemblages by using inter-species correlations and square root transformation of diatom percentages (Šmilauer and Lepš, 2014). PCA was performed using CANOCO 5 (ter Braak and Šmilauer, 2012).

3.3 Other paleolimnological proxies

Lake sediments' total carbon (TC) comprises endogenous and exogenous parts. The endogenous organic carbon is mainly contributed by the aquatic organisms (mainly plankton) of the lake, and the exogenous organic carbon is primarily contributed by the inland plants of the basin (Zhu et al., 2004). Total nitrogen (TN) reflects the nutrient status of the lake itself. Based on the restriction of TN on the nutrition of aquatic organisms, the C/N of lake sediments can better reflect the source of organic carbon in the sediments (Broiner and Mulvaney, 1982). Generally, the C/N of bacteria and algae is 4–10, while that of terrigenous vascular plants is above 20 (Lanzhou Institute of Geology, 1979; Meyers, 1994). To determine the effects of inferred catchment processes on diatom changes, TC, TN, and C/N data of core CGD were measured. TC and TN were determined by the EA300 Elemental Analyzer (Italy). The chemical index of alteration CIA was used to evaluate the weathering intensity of minerals in the sediment (Nesbitt and Young, 1982; $CIA = Al_2O_3 / (Al_2O_3 + K_2O + CaO) \times 100$). The geochemical element was determined by the ICP-AES Inductively Coupled Plasma Emission Spectrometer (US) as the

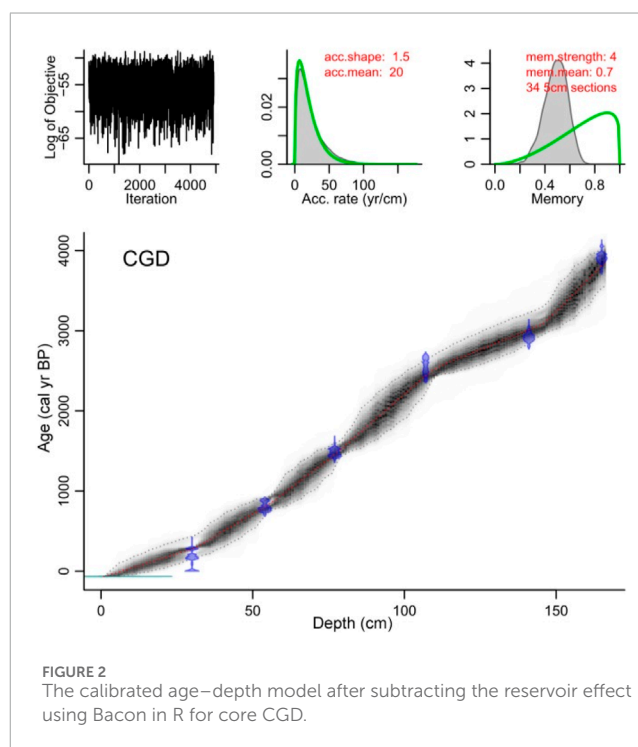


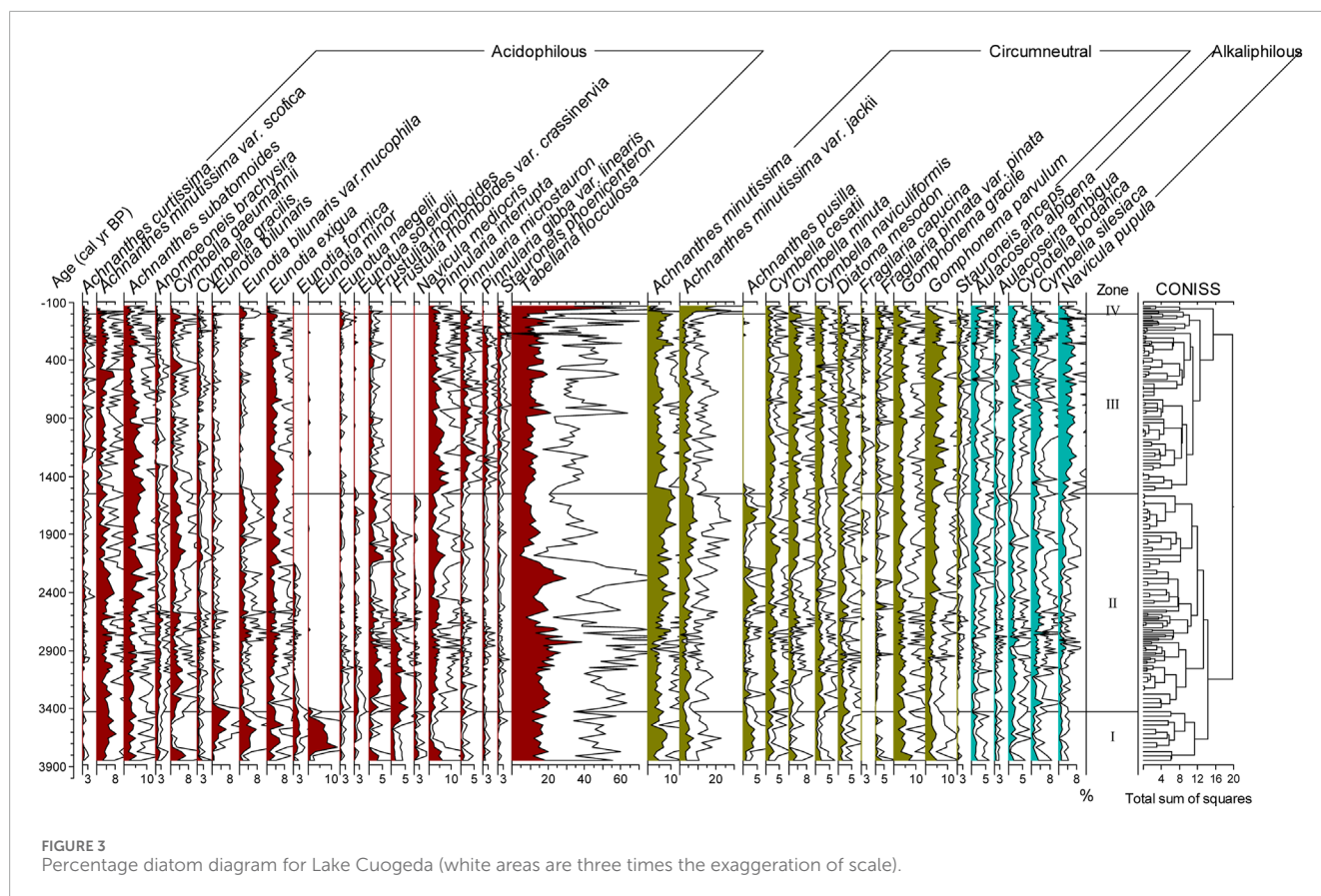
FIGURE 2 The calibrated age–depth model after subtracting the reservoir effect using Bacon in R for core CGD.

standard solution ($\pm 2\%$). This study used the element data of Al, K, and Ca.

4 Results

4.1 Chronology

An age–depth model based on the radiocarbon ages (Table 1) was constructed using the Bacon age model package (Blaauw and Christen, 2011; Figure 2). The top of the core is a fluffy layer preserved, so we considered the core top to be modern. From this age model, the bottom date was estimated to be 3850 cal yr BP (1900 BC), and the average time resolution of each sample was found to be ~24 years.



4.2 Diatom flora

The diatom assemblage is dominated by acidophilous and circumneutral oligotrophic small benthic taxa, such as *Tabellaria flocculosa*, *Achnanthes minutissima* var. *jackii*, *Achnanthes subatomoides*, *Eunotia minor*, *Eunotia bilunaris*, *Eunotia bilunaris* var. *mucophila*, *Eunotia exigua*, *Pinnularia interrupta*, *Achnanthes minutissima*, *Gomphonema gracile*, and *Gomphonema parvulum* (Supplementary Table S1). Some alkaliphilic benthic diatoms exist, for instance, *Navicula pupula* and *Cymbella silesiaca* (Supplementary Table S1). The content of planktic diatoms was very low, mainly *Aulacoseira alpigena* and *Cyclotella bodanica* (Figure 3). The average relative abundance of acidophilous diatom (ACD), circumneutral diatom (CD), and alkaliphilic diatom (ALD) species was 50.3%, 36.3%, and 10.3%, respectively (Figure 4). Based on CONISS results, the diatom assemblage was divided into four diatom biostratigraphic zones (Figure 3).

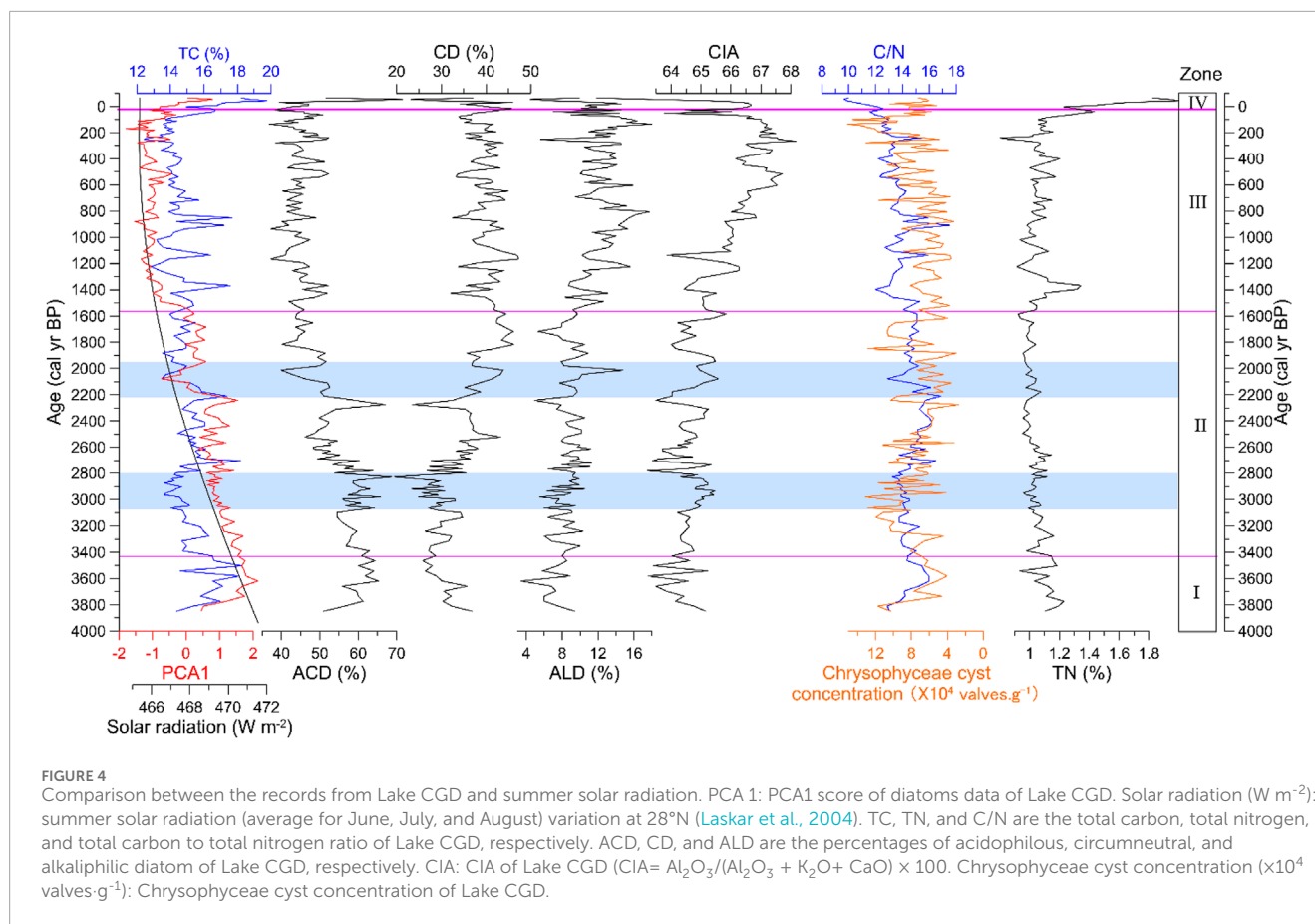
Zone I (166–155 cm, 3850–3430 cal yr BP (1900–1480 BC) was characterized by a relatively high abundance of ACD (58.8%), mainly contributed by *T. flocculosa* (11.7%–19.9%). *Gomphonema gracile*, *P. interrupta*, *Cymbella gaeumannii*, *Frustulia rhomboides*, *Caloneis lepidula*, *Pinnularia microstauron*, and *Navicula mediocris* exhibited their highest representation throughout the entire sequence during 3850–3755 cal yr BP (1900–1805 BC), and most

of those were circumneutral or slightly acidic species. From 3755 to 3430 cal yr BP (1805–1480 BC), the relative abundance of acidophilous *Eunotia* spp. reached the highest values of the entire core.

The relative abundance of ACD was down to 51.8% in zone II (155–80 cm, 3430–1550 cal yr BP (1480 BC–400 AD), and that was still characterized by a relatively high abundance of *T. flocculosa* (mean 14.9%). *Achnanthes minutissima*, *A. minutissima* var. *jackii*, *A. subatomoides*, *G. parvulum* and *G. gracile* were common in this zone. The average relative abundance of *Eunotia* species was generally reduced in this zone.

In Zone III (80–7 cm, 1550–3.6 cal yr BP (400–1946 AD), the acidophilous species *E. bilunaris* var. *mucophila*, *Eunotia formica*, *Frustulia rhomboides* var. *crassinervia*, *Navicula mediocris*, and circumneutral species *A. pusilla* almost disappeared. Except for *Pinnularia* spp., most of the acidophilous diatoms decreased and were replaced by an increase in the relative abundance of the alkaliphilic species *N. pupula*, *C. silesiaca* and *Cyclotella bodanica* and circumneutral species *G. parvulum*, *C. minuta*, *G. gracile*, *Cymbella naviculiformis*, *D. mesodon*, *Fragilaria pinnata* var. *pinnata*, and *Fragilaria capucina* var. *rumpens*.

In Zone IV (7–0 cm, 3.6–66 cal yr BP (1946–2016 AD), the mean relative abundances of *T. flocculosa* and *A. minutissima* var. *jackii* rose sharply to 29.3% and 14.2%, respectively.



4.3 Geophysical and chemical proxies

TC, TN, C/N, and CIA data from the CGD sediment core exhibited changes that generally correspond to the diatom assemblage zones (Figure 4). The mean content of TN was 1.05%, but it rose rapidly after 80 cal yr BP (1870 AD). The average content of TC was 15%; the C/N ratio changed between 9.6 and 17.5 (average 13.94). Both TC and C/N ratios fluctuated greatly and declined during the Late Holocene.

The average value of the CIA ranged from 61.5 to 68.2. It showed a gradually increasing trend from 3850 to 3.6 cal yr BP (1900 BC to 1946 AD) and is highly negatively correlated with ACD and positively correlated with ALD (Figure 4).

4.4 Autoecology of the main diatom taxa

After an extensive survey of the literature on diatom ecological preferences, we developed a list of diatom acidophilous, circumneutral, or alkaliphilic; see Supplementary Table S1. Most of the diatom species were oligotrophic acidophilous benthic species. The autecology of the main diatom taxa of Lake CGD is shown in Table 2.

The Chrysophyceae cyst has been proposed in high polar regions to estimate lake ice cover (Smol, 1983; Smol, 1988; Zeeb and Smol, 2001). Chrysophyceae can succeed in ice-covered

environments due to their versatile nutritional strategies, motility, and ability to form an excellent resting stage (Smol, 1983). Pelechata et al. (2015) showed that after mild winters, despite the higher availability of nutrients in lake water, the abundance and biomass of Chrysophyceae cysts are less numerous than after severe winters. Therefore, the Chrysophyceae cyst concentration of CGD may be an indirect proxy of lake ice cover.

4.5 Principal component analysis

The first two PCA axes of diatom abundances statistically explain 29.17% and 10.31% of the total variance, respectively (Figure 5), and the axes profiles are consistent with the diatom zones (Figure 4). The positive direction of the first axis is mainly associated with *F. rhomboides* var. *crassinervia*, *A. pusilla*, *Eunotia* spp., *N. mediocris*, *F. capucina* var. *rumpens*, *Anomoeoneis brachysira*, *T. flocculosa*, *A. minutissima* var. *scotica*, *A. ambigua*, and *F. rhomboides*. (Figure 5). The negative direction is mainly associated with *N. pupula*, *Stauroneis anceps*, *G. parvulum*, *C. minuta*, *P. microstauron*, *Fragilaria capucina*, *Stauroneis phoenicenteron*, *F. pinnata* var. *pinata*, *Pinnularia gibba* var. *linearis*, *C. naviculiformis*, *Achnanthes curtissima*, *P. interrupta*, *Neidium ampliatum*, and *A. alpigena* (Figure 5). The positive direction of the second axis is mainly associated with *E. minor*, *F. pinnata* var. *pinata*, *C. bodanica*, *A. minutissima* var. *jackii*, and *T. flocculosa*. The negative direction

TABLE 2 Autoecology of main diatom taxa from Lake Cuogeda.

Genus/Species	Autoecology	References
<i>Tabellaria flocculosa</i>	A colonial non-motile diatom consisting of an indefinite number of cells joined at their corners by mucilage pads that is usually abundant when water is turbulent	Knudson and Kipling. (1957), Whitmore. (1989)
Genus <i>Achnanthes</i>	It has a wide spectrum of ecological indicator values, but the average indicator value for the trophic state is relatively low	VanDam et al. (1994)
Genus <i>Eunotia</i>	Strong acidic and freshwater indicators prefer water bodies enriched with humic acids	VanDam et al. (1994); Glushchenko and Kulikovskiy. (2017)
<i>Gomphonema gracile</i>	A freshwater species that is tolerant of a wide range of pH and conductivity, preferring water of low nutrient content but also tolerating higher electrolyte brackish waters; it is a cosmopolitan species in standing water	Tobias and Gaiser. (2006)
<i>Gomphonema parvulum</i>	The indicator species of the environment at alkaline pH and standing waters. It is also considered common, cosmopolitan, and developing in large numbers in meso- to polysaprobic waters	Tobias and Gaiser. (2006); Klemenčič et al. (2010)
<i>Navicula pupula</i>	It is only standard in lakes with high pH and has been described as tolerant of moderate organic pollution	Lange-Bertalot. (1980); Rosén et al. (2000)

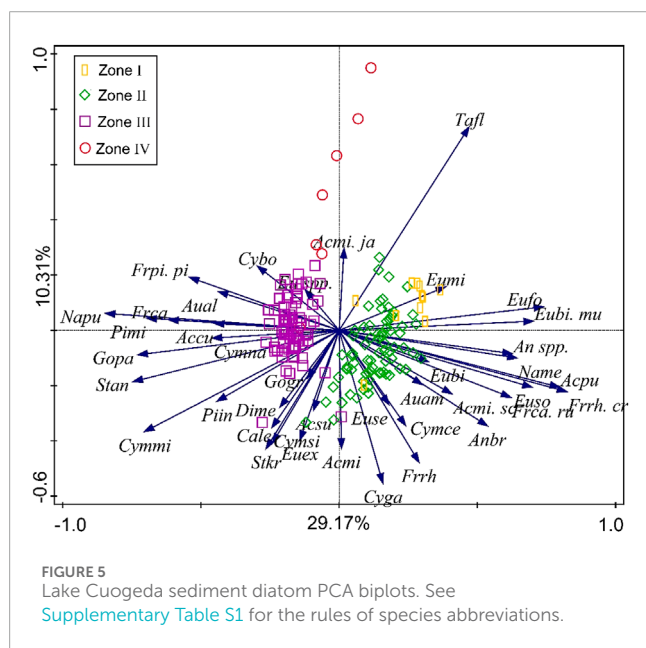


FIGURE 5 Lake Cuogeda sediment diatom PCA biplots. See Supplementary Table S1 for the rules of species abbreviations.

of the second axis is mainly associated with *C. gaeumannii*, *F. rhomboides*, *S. kriegeri*, *A. minutissima*, and *C. lepidula* (Figure 5).

The positive direction of the first axis of PCA is mainly associated with acidophilous diatoms and those who prefer humic acid and turbulent diatoms. At the same time, most of the alkaliphilic diatoms are located in the negative direction. Assemblage changes in the diatom of Lake Cuogeda record appear to be influenced by humic acids, turbulence, micro-habitat, and pH. Thus, PCA1 may not represent a single environmental gradient but a combination of gradients. An increased PCA1 score indicates an environment of higher humic acids and turbulence and lower pH. The

environmental factors of PCA2 were difficult to distinguish, so PCA2 was not discussed.

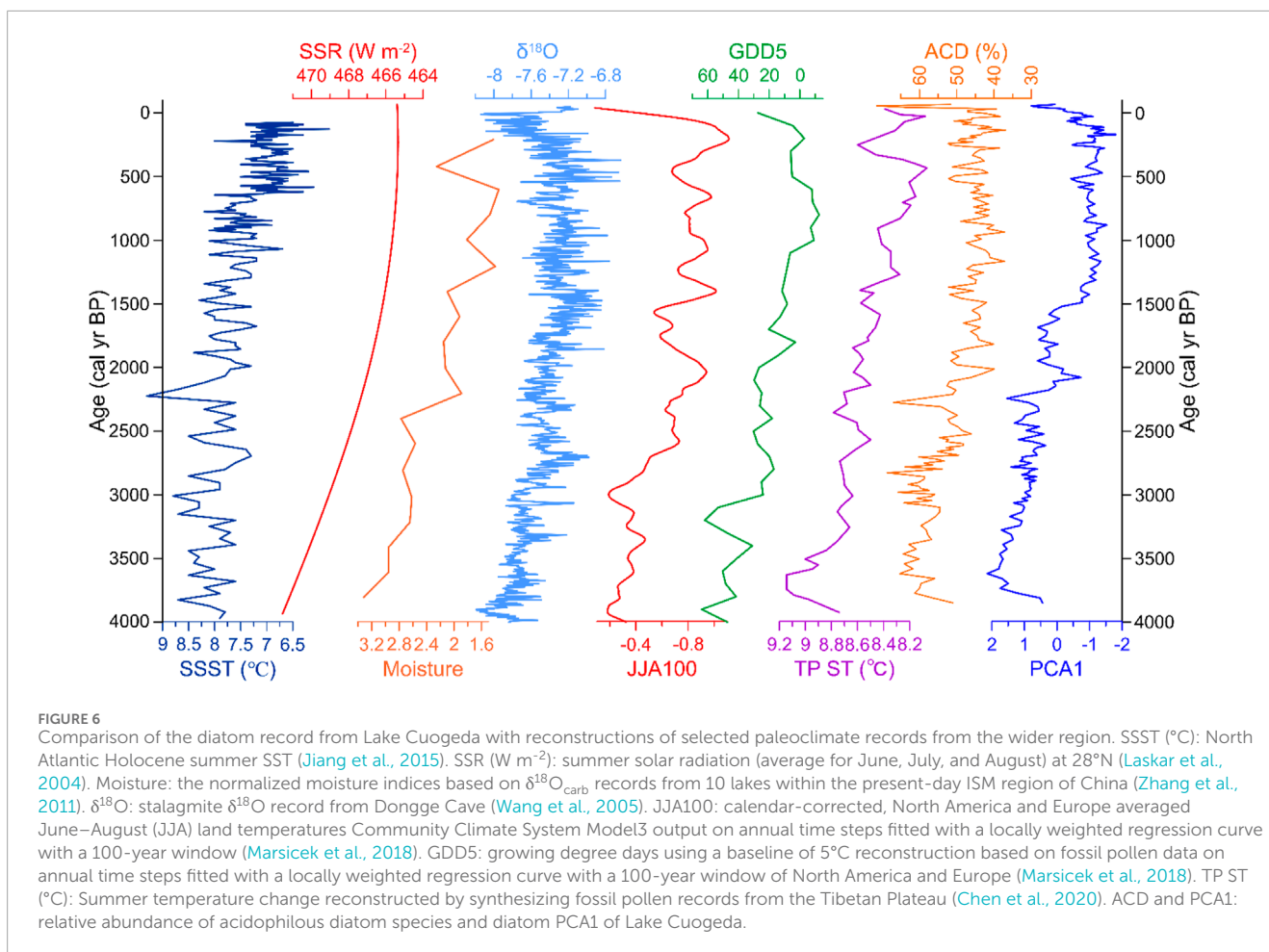
5 Discussion

5.1 Late Holocene paleoenvironment recorded in Lake Cuogeda

The interpretation of the paleoenvironment was mainly based upon the diatom assemblages, Chrysophyceae cyst concentration, and TN, TC, C/N, and CIA content of CGD. Those are plotted in Figures 3, 4.

From 3850 to 3430 cal yr BP (1900–1480 BC), the high value of PCA1 and *Eunotia* species reflects an acidic, oligotrophic, and enriched with a humic acids environment (Figures 3, 4; Glushchenko and Kulikovskiy, 2017; VanDam et al., 1994). The high value of C/N (Figure 4) indicates a high terrestrial humus supply to the lake. The low value of the Chrysophyceae cyst concentration reflects a relatively high temperature and short ice cover duration (Figure 4). Low CIA means weak erosion, weathering, and well-developed catchment soil (Figure 4; Fritz et al., 2004; Wolfe, 2003).

The percentage of *Eunotia* and ACD and the value of PCA1 decreased obviously from 3430 to 1550 cal yr BP (1480 BC to 400 AD) (Figures 3, 4), indicating less humic acid and relatively high pH. A relatively high Chrysophyceae cyst concentration reflects longer ice-cover duration and temperature drops than in the previous stage. The increase of CIA indicates a weakening of soil development, with increased cold climate erosion and weathering (Hu et al., 1993). A relatively cold, weathered watershed environment was identified from the relatively high CIA and Chrysophyceae cyst concentration at ~2800 cal yr BP (850 BC) (Figure 4). At that time, the relatively low PCA1, TC, TN, and C/N reflect a moderately alkaline lake environment and decreased nutrient input in the basin (Figure 4). This may respond to Bond event 2 (Bond et al., 1997; Plunkett and



Swindles, 2008). Between 2210 and 1950 cal yr BP (260 BC to 0 AD), there was a relatively cold and weathered watershed environmental fluctuation that was recorded with high CIA and Chrysophyceae cyst concentration (Figure 4), which was related to weak ISM. This was accompanied by a relatively alkaline lake environment and the decrease of nutrient input in the basin, reflected by the relatively low PCA1, TC, TN, and C/N from 2210 to 1950 cal yr BP (260 BC to 0 AD) (Figure 4). The diatoms of Tiancai Lake (~3898 m asl) in Yunnan also showed a weak monsoon fluctuation at a similar time (Chen et al., 2014).

From 1550 to 3.6 cal yr BP (400–1946 AD), some acidophilous diatom species almost disappeared and were replaced by alkaliphilic species (Figure 3). This indicates that the lake ecosystem has changed to a higher pH condition. The relatively high percentage of CD and ALD also show relatively high pH (Figure 4). The rising pH corresponds to the rising CIA because bedrock weathering and erosion processes will carry alkalinity and base cations into the lake (Figure 4). Chrysophyceae cyst concentration gradually increased (Figure 4), reflecting low temperature and a prolonged freezing time.

From 3.6 cal yr BP (1946 AD) to the present, the diatom species have shifted toward a higher relative abundance of acidophilous diatoms, and the value of PCA1 is also high (Figures 3, 4). The relative abundance of *T. flocculosa* is very high; the

Chrysophyceae cyst concentration is relatively low (Figures 3, 4). Those are consistent with an environment of shorter duration of ice cover and stronger lake water turbulence (Rühland et al., 2003). Recent anthropogenic warming may be vital in influencing diatom community composition and lake water dynamics after 3.6 cal yr BP (1946 AD) (Catalan et al., 2002; Koinig et al., 2002; Rühland et al., 2015).

5.2 Comparison with regional climate records and possible mechanisms

Regarding the overall trend, PCA1, ACD, TC, and Chrysophyceae cyst concentration of Lake CGD decreased, while CD, ALD, and CIA increased during the past ~4000 years (Figure 4). These environmental proxies indicate that the content of exogenous humic acid and turbulence of lake water showed a downward trend. In contrast, the lake water's pH, ice-cover duration, and basin weathering showed an upward trend. As an area affected by the ISM, these phenomena comprehensively reflect the decreasing trend of the ISM strength during the past ~4000 years. This trend is consistent with other records from the Tibetan Plateau, such as the quantitative summer temperature reconstruction based on subfossil chironomids from Tiancai Lake on the SE edge

of the Tibetan Plateau (Zhang et al., 2017); the pollen-based mean July temperature reconstruction from Xingyun Lake on the SE edge of the Tibetan Plateau (Wu et al., 2018); summer temperature variations reconstructed from a synthesis of fossil pollen records from the Tibetan Plateau (Figure 6) (Chen et al., 2020); and a decreasing trend over the past ~4000 years that has also been reported by the temperature record from Xiada Co on the western Tibetan Plateau (Li et al., 2024). Our records are also well correlated with the June–August land temperature reconstruction and growing degree days (using a baseline of 5°C) reconstruction for North America and Europe (Figure 6) (Marsicek et al., 2018).

Notably, the decreasing trend of the ISM strength recorded by Lake CGD shows strong similarities with other high-resolution summer monsoon records (Marcott et al., 2013). It is generally correlated to increases in $\delta^{18}\text{O}$ records from Dongge Cave (Figure 6), which is interpreted as a reduction in summer monsoon strength (Wang et al., 2005). It is also generally correlated to the normalized moisture indices based on $\delta^{18}\text{O}_{\text{carb}}$ records from 10 lakes within the present-day ISM region of China, which show that the ISM gradually weakened in the Late Holocene (Zhang et al., 2011) (Figure 6). A decreasing trend of the ISM strength over the past ~4000 years has also been reported by the record from Hongyuan Pea on the Tibetan Plateau (Hong et al., 2003). The precisely dated and well-calibrated tree-ring stable isotope chronology from the Tibetan Plateau also reflects a rapid decrease in ISM since the mid-Holocene (Yang et al., 2021). Therefore, the environmental evolution recorded by our diatoms over the Late Holocene is generally associated with decreased ISM intensity (Hou et al., 2015; Wu et al., 2018; Chen et al., 2020).

Studies have indicated physical links between the Atlantic Multidecadal Oscillation and the multidecadal variability of the ISM (Goswami et al., 2006). North Atlantic SST anomalies strongly affect the Tibetan Plateau surface temperature and heat sources (Feng and Hu, 2008). The decreasing trend of the ISM strength over the past ~4000 years, recorded by Lake CGD, is associated with North Atlantic Holocene summer SSTs (Figure 6) (Jiang et al., 2015). It means a correlation exists between the North Atlantic SSTs and the trend of environmental change in the study area. The decrease of the ISM strength recorded by Lake CGD also generally follows summer solar radiation in the northern hemisphere (Figure 6), indicating that insolation has a significant influence on environmental change in the study region (Laskar et al., 2004; Gupta et al., 2005). North Atlantic SST change and solar activity may be key driving factors of environmental change in the study area (Keyimu et al., 2021).

6 Conclusion

To better understand how the global and regional-scale environment has changed during the Holocene, it is essential to conduct paleoenvironment research with sufficient spatiotemporal resolution. Sedimentary diatoms of Lake Cuogeda were analyzed to track the environmental variations of SW China over the past 4000 years. An age–depth model was established using AMS ^{14}C dating techniques on five plant remains and 1 moss.

Diatom and other geochemical proxies show that, from 3850 to 3430 cal yr BP (1900–1480 BC), the environment of Lake CGD was acidic, oligotrophic, and enriched with humic acids, and the lake ice-cover duration was short. During 3430–1550 cal yr BP (1480 BC–400 AD), Lake CGD had less humic acid and a relatively high pH environment. A relatively high Chrysophyceae cyst concentration reflected longer ice-cover duration and temperature drops. Our multi-indicator recorded two environmental fluctuations at ~2800 cal yr BP (850 BC) and 2210–1950 cal yr BP (260 BC–0 AD). From 1550 to 3.6 cal yr BP (400–1946 AD), the lake ecosystem changed to a higher pH condition. Chrysophyceae cyst concentration gradually increased in this period, reflecting low temperature and a prolonged freezing time. From 3.6 cal yr BP (1946 AD) to the present, Lake CGD's water has been acidic, with an environment of shorter duration of ice cover and stronger lake water turbulence.

The environmental proxies of Lake CGD comprehensively reflect a decreasing trend of the ISM strength during the past ~4000 years. This trend follows the decreasing trend of regional and global summer temperature reconstructions and shows strong similarities to other high-resolution ISM records. North Atlantic SST change and solar activity may be key driving factors of environmental change over the study area.

Data availability statement

The raw data supporting the conclusion of this article will be made available by the authors, without undue reservation.

Author contributions

YZ: Conceptualization, Data curation, Formal Analysis, Investigation, Methodology, Project administration, Software, Visualization, Writing–original draft, Writing–review and editing. WP: Writing–review and editing. YL: Methodology, Project administration, Resources, Supervision, Writing–review and editing. XX: Project administration, Resources, Supervision, Writing–review and editing. AH: Writing–review and editing.

Funding

The author(s) declare financial support was received for the research, authorship, and/or publication of this article. This work was supported by the National Natural Science Foundation of China (41672173), the National Key R&D Program of China (2016YFA0600501), and the National Natural Science Foundation of China (41877296, 41572149, and 41877434). The Suzhou Chien-Shiung Institute of Technology doctoral research fund supported the open access publication fee.

Acknowledgments

We thank John P. Smol for improving the manuscript and language.

Conflict of interest

The authors declare that the research was conducted in the absence of any commercial or financial relationships that could be construed as a potential conflict of interest.

The reviewer XL declared a shared affiliation with the author YL to the handling editor at time of review.

Publisher's note

All claims expressed in this article are solely those of the authors and do not necessarily represent those of

their affiliated organizations, or those of the publisher, the editors and the reviewers. Any product that may be evaluated in this article, or claim that may be made by its manufacturer, is not guaranteed or endorsed by the publisher.

Supplementary material

The Supplementary Material for this article can be found online at: <https://www.frontiersin.org/articles/10.3389/feart.2024.1324724/full#supplementary-material>

References

- An, Z., Clemens, S. C., Shen, J., Qiang, X., Jin, Z., Sun, Y., et al. (2011). Glacial-interglacial Indian summer monsoon dynamics. *Science* 333, 719–723. doi:10.1126/science.1203752
- Battarbee, R. W., Jones, V. J., Flower, R. J., Cameron, N. G., Bennion, H., Carvalho, L., et al. (2002). "Diatoms," in *Tracking environmental change using lake sediments*. Editors J. P. Smol, H. J. B. Birks, and W. M. E. Last (Dordrecht: Kluwer Academic Publisher), 155–202.
- Bigler, C., and Hall, R. I. (2003). Diatoms as quantitative indicators of July temperature: a validation attempt at century-scale with meteorological data from northern Sweden. *Palaeogeogr. Palaeoclimatol. Palaeoecol.* 189, 147–160. doi:10.1016/S0031-0182(02)00638-7
- Bird, B. W., Polisar, P. J., Yanbin, L., Thompson, L. G., Yao, T., Finney, B. P., et al. (2014). A Tibetan lake sediment record of Holocene Indian summer monsoon variability. *Earth Planet. Sci. Lett.* 399, 92–102. doi:10.1016/j.epsl.2014.05.017
- Blaauw, M., and Christen, J. (2011). Flexible paleoclimate age–depth models using an autoregressive gamma process. *Bayesian. Anal.* 6, 457–474. doi:10.1214/11-BA618
- Bond, G., Showers, W., Cheseby, M., Lotti, R., Almasi, P., deMenocal, P., et al. (1997). A pervasive millennial-scale cycle in North Atlantic Holocene and glacial climates. *Science* 278, 1257–1266. doi:10.1126/science.278.5341.1257
- Broiner, I. M., and Mulvaney, C. S. (1982). "Nitrogen-total," in *Methods of soil analysis, Part 2 chemical and microbiological properties*. Editor A. L. Page (Madison, Wisconsin USA: American Society of Agronomy, Inc), 595–624.
- Catalan, J., Pla, S., Rieradevall, M., Felip, M., Ventura, M., Buchaca, T., et al. (2002). Lake Redó ecosystem response to an increasing warming the Pyrenees during the twentieth century. *J. Paleolimnol.* 28, 129–145. doi:10.1023/A:1020380104031
- Chen, D. L., Xu, B. Q., Yao, T. D., Guo, Z. T., Cui, P., Chen, F. H., et al. (2015). Assessment of past, present and future environmental changes on the Tibetan Plateau. *Chin. Sci. Bull.* 60, 3025–3035. doi:10.1360/n972014-01370
- Chen, F., Chen, X., Chen, J., Zhou, A., Wu, D. U. O., Tang, L., et al. (2014a). Holocene vegetation history, precipitation changes and Indian Summer Monsoon evolution documented from sediments of Xingyun Lake, south-west China. *J. Quat. Sci.* 29, 661–674. doi:10.1002/jqs.2735
- Chen, F., Zhang, J., Liu, J., Cao, X., Hou, J., Zhu, L., et al. (2020). Climate change, vegetation history, and landscape responses on the Tibetan plateau during the holocene: a comprehensive review. *Quat. Sci. Rev.* 243, 106444–106521. doi:10.1016/j.quascirev.2020.106444
- Chen, X., Li, Y., Metcalfe, S., Xiao, X., Yang, X., and Zhang, E. (2014b). Diatom response to Asian monsoon variability during the Late Glacial to Holocene in a small treeline lake, SW China. *Holocene* 24, 1369–1377. doi:10.1177/0959683614540951
- Cui, A., Lv, H., Liu, X., Shen, C., Xu, D., Xu, B., et al. (2021). Tibetan plateau precipitation modulated by the periodically coupled westerlies and asian monsoon. *Geophys. Res. Lett.* 48, e2020GL091543. doi:10.1029/2020GL091543
- Feng, S., and Hu, Q. (2008). How the North Atlantic Multidecadal Oscillation may have influenced the Indian summer monsoon during the past two millennia. *Geophys. Res. Lett.* 35. doi:10.1029/2007GL032484
- Fritz, S. C., and Anderson, N. J. (2013). The relative influences of climate and catchment processes on Holocene lake development in glaciated regions. *J. Quat. Sci.* 49, 349–362. doi:10.1007/s10933-013-9684-z
- Fritz, S. C., Engstrom, D. R., and Juggins, S. (2004). Patterns of early lake evolution in boreal landscapes: a comparison of stratigraphic inferences with a modern chronosequence in Glacier Bay, Alaska. *Holocene* 14, 828–840. doi:10.1191/0959683604hl763rp
- Glushchenko, A. M., and Kulikovskiy, M. S. (2017). Taxonomy and distribution of the genus *Eunotia* Ehrenberg in aquatic ecosystems of Vietnam. *Inland Water Biol.* 10, 130–139. doi:10.1134/S1995082917020055
- Goswami, B. N., Madhusoodanan, M. S., Neema, C. P., and Sengupta, D. (2006). A physical mechanism for North Atlantic SST influence on the Indian summer monsoon. *Geophys. Res. Lett.* 33. doi:10.1029/2005GL024803
- Grimm, E. C. (1987). CONISS: a FORTRAN 77 program for stratigraphically constrained cluster analysis by the method of incremental sum of squares. *Comput. Geosci.* 13, 13–35. doi:10.1016/0098-3004(87)90022-7
- Grimm, E. C. (2004). *TILIA and TGView software*. Illinois state museum. United States: Research and Collection Center.
- Gupta, A. K., Das, M., and Anderson, D. M. (2005). Solar influence on the Indian summer monsoon during the Holocene. *Geophys. Res. Lett.* 32, 1–4. doi:10.1029/2005GL022685
- Hillman, A. L., Abbott, M. B., Finkenbinder, M. S., and Yu, J. (2017). An 8,600 year lacustrine record of summer monsoon variability from Yunnan, China. *Quat. Sci. Rev.* 174, 120–132. doi:10.1016/j.quascirev.2017.09.005
- Hillman, A. L., Campisi, A. N., Abbott, M. B., Bain, D. J., Bain, M. P., Tisherman, R. A., et al. (2022). Yilong lake level record documents coherent regional-scale changes in Holocene water balance in Yunnan, southwestern China. *Palaeogeogr. Palaeoclimatol. Palaeoecol.* 601, 111148. doi:10.1016/j.palaeo.2022.111148
- Hong, Y. T., Hong, B., Lin, Q. H., Zhu, Y. X., Shibata, Y., Hirota, M., et al. (2003). Correlation between Indian ocean summer monsoon and North Atlantic climate during the holocene. *Earth. Planet. Sci. Lett.* 211, 371–380. doi:10.1016/S0012-821X(03)00207-3
- Hou, J., Huang, Y., Zhao, J., Liu, Z., Colman, S., and An, Z. (2015). Large Holocene summer temperature oscillations and impact on the peopling of the northeastern Tibetan Plateau. *Geophys. Res. Lett.* 43, 1323–1330. doi:10.1002/2015GL067317
- Hu, F. S., Brubaker, L. B., and Anderson, P. M. (1993). A 12 000 year record of vegetation change and soil development from Wien Lake, central Alaska. *Can. J. Bot.* 71, 1133–1142. doi:10.1139/b93-133
- Jiang, H., Muscheler, R., Björck, S., Seidenkrantz, M. S., Olsen, J., Sha, L., et al. (2015). Solar forcing of Holocene summer sea-surface temperatures in the northern North Atlantic. *Geology* 43, 203–206. doi:10.1130/G36377.1
- Jiménez, L., Conde-Porcuna, J. M., García-Alix, A., Toney, J. L., Anderson, R. S., Heiri, O., et al. (2019). Ecosystem responses to climate-related changes in a mediterranean alpine environment over the last ~ 180 years. *Ecosystems* 22, 563–577. doi:10.1007/s10021-018-0286-5
- Keyimu, M., Li, Z., Liu, G., Fu, B., Fan, Z., Wang, X., et al. (2021). Tree-ring based minimum temperature reconstruction on the southeastern Tibetan Plateau. *Quat. Sci. Rev.* 251, 106712. doi:10.1016/j.quascirev.2020.106712
- Klemenčič, A. K., Smolar-Žvanut, N., Istenič, D., and Griessler-Bulc, T. (2010). Algal community patterns in Slovenian bogs along environmental gradients. *Biologia* 65, 422–437. doi:10.2478/s11756-010-0033-7
- Knudson, B. M., and Kipling, T. H. (1957). Ecology of the epiphytic diatom *Tabellaria flocculosa* (roth) kutz. Var. *Flocculosa* in three English lakes. *J. Ecol.* 45, 93–112. doi:10.2307/2257078
- Koinig, K. A., Kamenik, C., Schmidt, R., Agustí-Panareda, A., Appleby, P., Lami, A., et al. (2002). Environmental changes in an alpine lake (Gossenköllesee, Austria) over the last two centuries – the influence of air temperature on biological parameters. *J. Paleolimnol.* 28, 147–160. doi:10.1023/A:1020332220870
- Kramer, A., Herzsich, U., Mischke, S., and Zhang, C. (2010). Holocene treeline shifts and monsoon variability in the Hengduan Mountains (southeastern Tibetan

- Plateau), implications from palynological investigations. *Palaeogeogr. Palaeoclimatol. Palaeoecol.* 286, 23–41. doi:10.1016/j.palaeo.2009.12.001
- Krammer, K., and Lange-Bertalot, H. (1986). “Bacillariophyceae 1. Teil: naviculaceae,” in *Süsswasserflora von Mitteleuropa 2/1*. Editors H. Ettl, G. Gärtner, J. Gerloff, H. Heynig, and D. E. Mollenhauer (Jena, Germany: Gustav Fischer Verlag), 1–596.
- Krammer, K., and Lange-Bertalot, H. (1988). “Bacillariophyceae 2. Teil: bacillariaceae, epithemiaceae, surirellaceae,” in *Süsswasserflora von Mitteleuropa 2/2*. Editors H. Ettl, G. Gärtner, J. Gerloff, H. Heynig, and D. E. Mollenhauer (Jena, Germany: Gustav Fischer Verlag), 1–576.
- Krammer, K., and Lange-Bertalot, H. (1991a). “Bacillariophyceae 3. Teil: centrales, fragilariaceae, eunotiaceae,” in *Süsswasserflora von Mitteleuropa 2/3*. Editors H. Ettl, G. Gärtner, J. Gerloff, H. Heynig, and D. E. Mollenhauer (Jena, Germany: Gustav Fischer Verlag), 1–576.
- Krammer, K., and Lange-Bertalot, H. (1991b). “Bacillariophyceae 4. Teil: achnanthaceae, Kritische Ergänzungen zu Navicula (Lineolate) und Gomphonema,” in *Süsswasserflora von Mitteleuropa 2/4*. Editors H. Ettl, G. Gärtner, J. Gerloff, H. Heynig, and D. E. Mollenhauer (Jena, Germany: Gustav Fischer Verlag), 1–437.
- Lange-Bertalot, H. (1980). Zur taxonomischen Revision einiger ökologisch wichtiger Naviculaceae lineolatae Cleve. Die Formenkreise um Navicula lanceolata, N. viridula, N. cari. *Cryptogam. Algol.* 1, 29–50.
- Lanzhou Institute of Geology (1979). *Integrated investigation reports of oinghai lake*. Bering: Science Press, 156–169.
- Larocque, I., and Bigler, C. (2004). Similarities and discrepancies between chironomid- and diatom-inferred temperature reconstructions through the Holocene at Lake 850, northern Sweden. *Quatern. Int.* 122, 109–121. doi:10.1016/j.quaint.2004.01.033
- Laskar, J., Robutel, P., Joutel, F., Gastineau, M., Correia, A. C. M., and Levrard, B. (2004). A long-term numerical solution for the insolation quantities of the Earth. *Astron. Astrophys.* 428, 261–285. doi:10.1051/0004-6361:20041335
- Li, X., Liu, S., Ji, K., Hou, X., Yuan, K., Hou, J., et al. (2024). Late Holocene human population change revealed by fecal stanol records and its response to environmental evolution at Xiada Co on the western Tibetan Plateau. *Palaeogeogr. Palaeoclimatol. Palaeoecol.* 636, 111993. doi:10.1016/j.palaeo.2023.111993
- Li, X., Zhang, Y., Hou, J., Wang, M., Fan, B., Yan, J., et al. (2022). Spatio-temporal patterns of centennial-scale climate change over the Tibetan Plateau during the past two millennia and their possible mechanisms. *Quat. Sci. Rev.* 292, 107664. doi:10.1016/j.quascirev.2022.107664
- Li, Y., Chen, X., Xiao, X., Zhang, H., Xue, B., Shen, J., et al. (2018). Diatom-based inference of Asian monsoon precipitation from a volcanic lake in southwest China for the last 18.5 ka. *Quat. Sci. Rev.* 182, 109–120. doi:10.1016/j.quascirev.2017.11.021
- Liu, X., Yu, Z., Dong, H., and Chen, H. F. (2014). A less or more dusty future in the Northern Qinghai-Tibetan Plateau? *Sci. Rep.* 4, 6672. doi:10.1038/srep06672
- Lotter, A. F., Pienitz, R., and Schmidt, R. (2010). “Diatoms as indicators of environmental change in subarctic and alpine regions,” in *The diatoms: applications for the environmental and Earth Sciences*. Editors E. F. Stoermer, and J. P. Smol (Cambridge: Cambridge University Press), 231–248.
- Ma, H. H. (2013). Petrology and geochemical characteristics of laojunshan granite in southeast yunnan and its tectonic significance. (Master thesis). Beijing, China: China University of Geosciences.
- Marcott, S. A., Shakun, J. D., Clark, P. U., and Mix, A. C. (2013). A reconstruction of regional and global temperature for the past 11,300 years. *Science* 1198, 1198–1201. doi:10.1126/science.1228026
- Marsicek, J., Shuman, B. N., Bartlein, P. J., Shafer, S. L., and Brewer, S. (2018). Reconciling divergent trends and millennial variations in Holocene temperatures. *Nature* 554, 92–96. doi:10.1038/nature25464
- Meyers, P. A. (1994). Preservation of elemental and isotopic source identification of sedimentary organic matter. *Chem. Geol.* 114, 289–302. doi:10.1016/0009-2541(94)90059-0
- Nesbitt, H. W., and Young, G. M. (1982). Early Proterozoic climates and plate motions inferred from major element chemistry of lutites. *Nature* 299, 715–717. doi:10.1038/299715a0
- Pelechata, A., Pelechaty, M., and Pukacz, A. (2015). Winter temperature and shifts in phytoplankton assemblages in a small Chara-lake. *Aquat. Bot.* 124, 10–18. doi:10.1016/j.aquabot.2015.03.001
- Plunkett, G., and Swindles, G. T. (2008). Determining the Sun’s influence on Lateglacial and Holocene climates: a focus on climate response to centennial-scale solar forcing at 2800 cal. BP. *Quat. Sci. Rev.* 27, 175–184. doi:10.1016/j.quascirev.2007.01.015
- Rosén, P., Hall, R., Korsman, T., and Renberg, I. (2000). Diatom transfer-functions for quantifying past air temperature, pH and total organic carbon concentration from lakes in northern Sweden. *J. Paleolimnol.* 24, 109–123. doi:10.1023/A:1008128014721
- Rühland, K., Priesnitz, A., and Smol, J. P. (2003). Paleolimnological evidence from diatoms for recent environmental changes in 50 lakes across Canadian arctic treeline. *Arct. Antarct. Alp. Res.* 35, 110–123. doi:10.1657/1523-0430(2003)035[0110:pefdfr]2.0.co;2
- Rühland, K. M., Paterson, A. M., and Smol, J. P. (2015). Lake diatom responses to warming: reviewing the evidence. *J. Paleolimnol.* 54, 1–35. doi:10.1007/s10933-015-9837-3
- Salmaso, N. (2005). Effects of climatic fluctuations and vertical mixing on the interannual trophic variability of Lake Garda, Italy. *Limnol. Oceanogr.* 50, 553–565. doi:10.4319/lo.2005.50.2.0553
- Shi, J. P. (2007). Community ecology and biogeography of the mossy dwarf forest in yunnan. PhD thesis. Kunming, China: Xishuangbanna Tropical Botanical Garden, Chinese Academy of Sciences.
- Šmilauer, P., and Lepš, J. (2014). *Multivariate analysis of ecological data using CANOCO 5*. Cambridge: Cambridge University Press.
- Smol, J. P. (1983). Paleophycology of a high arctic lake near cape herschel, ellesmere island. *Can. J. Bot.* 61, 2195–2204. doi:10.1139/b83-238
- Smol, J. P. (1988). Chrysophycean microfossils in paleolimnological studies. *Palaeogeogr. Palaeoclimatol. Palaeoecol.* 62, 287–297. doi:10.1016/0031-0182(88)90058-2
- Sommaruga-Wögrath, S., Koinig, K. A., Schmidt, R., Sommaruga, R., Tessadri, R., and Psenner, R. (1997). Temperature effects on the acidity of remote alpine lakes. *Nature* 387, 64–67. doi:10.1038/387064a0
- Stoermer, E. F., and Smol, J. P. (1999). “Applications and uses of diatoms: prologue,” in *The diatoms: applications for the environmental and Earth Sciences*. Editors E. F. Stoermer, and J. P. Smol (Cambridge: Cambridge University Press), 3–8.
- Stuiver, M., Reimer, P. J., and Reimer, R. W. (2020). CALIB 8.2. Available at: <http://calib.org>.
- ter Braak, C. J. F., and Smilauer, P. (2012). *Canoco reference manual and user’s guide: software for ordination, version 5.0*. Ithaca USA: Microcomputer Power, p496.
- Tobias, F. A. C., and Gaiser, E. E. (2006). Taxonomy and distribution of diatoms in the genus Gomphonema from the Florida Everglades, USA. *Diatom Res.* 21, 379–405. doi:10.1080/0269249x.2006.9705677
- VanDam, H., Mertens, A., and Sinkeldam, J. (1994). A coded checklist and ecological indicator values of freshwater diatoms from The Netherlands. *J. Aquat. Ecol.* 28, 117–133. doi:10.1007/BF02334251
- Von Gunten, L., Heiri, O., Bigler, C., Van Leeuwen, J., Casty, C., Lotter, A. F., et al. (2008). Seasonal temperatures for the past~ 400 years reconstructed from diatom and chironomid assemblages in a high-altitude lake (Lej da la Tschappa, Switzerland). *J. Paleolimnol.* 39, 283–299. doi:10.1007/s10933-007-9103-4
- Wang, H., Hong, Y., Lin, Q., Hong, B., Zhu, Y., Wang, Y., et al. (2010). Response of humification degree to monsoon climate during the Holocene from the Hongyuan peat bog, eastern Tibetan Plateau. *Palaeogeogr. Palaeoclimatol. Palaeoecol.* 286, 171–177. doi:10.1016/j.palaeo.2009.12.015
- Wang, Y. J., Cheng, H., Edwards, R. L., He, Y. Q., Kong, X. G., An, Z. S., et al. (2005). The holocene asian monsoon links to solar changes and North Atlantic climate. *Science* 308, 854–857. doi:10.1126/science.1106296
- Whitmore, T. J. (1989). Florida diatom assemblages as indicators of trophic state and pH. *Limnol. Oceanogr.* 34, 882–895. doi:10.4319/lo.1989.34.5.0882
- Wolfe, A. P. (2003). Diatom community responses to late-Holocene climatic variability, Baffin Island, Canada: a comparison of numerical approaches. *Holocene* 13, 29–37. doi:10.1191/0959683603hl592rp
- Wu, D., Chen, X., Lv, F., Brenner, M., Curtis, J., Zhou, A., et al. (2018). Decoupled early Holocene summer temperature and monsoon precipitation in southwest China. *Quat. Sci. Rev.* 193, 54–67. doi:10.1016/j.quascirev.2018.05.038
- Wu, X., Dong, H., Zhang, C. L., Liu, X., Hou, W., Zhang, J., et al. (2013). Evaluation of glycerol dialkyl glycerol tetraether proxies for reconstruction of the paleoenvironment on the Qinghai-Tibetan Plateau. *Org. Geochem.* 61, 45–56. doi:10.1016/j.orggeochem.2013.06.002
- Wu, Z., Zhu, Y., and Jiang, H. (1987). *Vegetation of yunnan province*. Beijing, China: Science Press.
- Xiao, X. Y., Shen, J., and Wang, S. M. (2011). Spatial variation of modern pollen from surface lake sediments in Yunnan and southwestern Sichuan Province, China. *Rev. Palaeobot. Palynol.* 165, 224–234. doi:10.1016/j.revpalbo.2011.04.001
- Xu, H., Zhou, X., Lan, J., Liu, B., Sheng, E., Yu, K., et al. (2015). Late holocene Indian summer monsoon variations recorded at Lake erhai, southwestern China. *Quatern. Res.* 83, 307–314. doi:10.1016/j.yqres.2014.12.004
- Yang, J., Xia, D., Gao, F., Wang, S., Li, D., Fan, Y., et al. (2021). Holocene moisture evolution and its response to atmospheric circulation recorded by aeolian deposits in the southern Tibetan Plateau. *Quat. Sci. Rev.* 270, 107169. doi:10.1016/j.quascirev.2021.107169
- Yao, Y. F., Song, X. Y., Wortley, A. H., Wang, Y. F., Blackmore, S., and Li, C. S. (2017). Pollen-based reconstruction of vegetational and climatic change over the past ~30 ka

at Shudu Lake in the Hengduan Mountains of Yunnan, southwestern China. *PLoS One* 12, e0171967. doi:10.1371/journal.pone.0171967

Zeeb, B. A., and Smol, J. P. (2001). "Chrysophyte scales and cysts," in *Tracking environmental change using lake sediments volume 3: terrestrial, algal, and siliceous indicators*. Editors J. P. Smol, H. J. B. Birks, and W. M. Last (Dordrecht, Netherlands: Kluwer Academic Publishers), 203–225. doi:10.1007/0-306-47668-1_9

Zhang, C., Zhao, C., Yu, S. Y., Xue, B., Yang, X. D., Li, Y. L., et al. (2023). Divergent trends of changes in annual mean and summer temperature in southwestern China during the Holocene. *Glob. Planet. Change* 228, 104218. doi:10.1016/j.gloplacha.2023.104218

Zhang, E., Chang, J., Cao, Y., Sun, W., Shulmeister, J., Tang, H., et al. (2017). Holocene high-resolution quantitative summer temperature reconstruction based on subfossil chironomids from the southeast margin of the Qinghai-Tibetan Plateau. *Quat. Sci. Rev.* 165, 1–12. doi:10.1016/j.quascirev.2017.04.008

Zhang, J., Chen, F., Holmes, J. A., Li, H., Guo, X., Wang, J., et al. (2011). Holocene monsoon climate documented by oxygen and carbon isotopes from lake sediments and peat bogs in China: a review and synthesis. *Quat. Sci. Rev.* 30, 1973–1987. doi:10.1016/j.quascirev.2011.04.023

Zhao, C., Liu, Z., Rohling, E. J., Yu, Z., Liu, W., He, Y., et al. (2013). Holocene temperature fluctuations in the northern Tibetan Plateau. *Quat. Res.* 80, 55–65. doi:10.1016/j.yqres.2013.05.001

Zheng, Y., Li, Q., Wang, Z., Naafs, B. D. A., Yu, X., and Pancost, R. D. (2015). Peatland GDGT records of Holocene climatic and biogeochemical responses to the Asian Monsoon. *Org. Geochem.* 87, 86–95. doi:10.1016/j.orggeochem.2015.07.012

Zhu, L., Wang, J., Chen, L., Yang, J., Li, B., Zhu, Z., et al. (2004). 20,000-year environmental change reflected by multidisciplinary lake sediments in Chen Co, Southern Tibet. *Acta Geogr. sin.* 59, 514–524.